Invited Paper

TUTORIAL ON ADVANCES IN MORPHOLOGICAL IMAGE PROCESSING AND ANALYSIS

Petros Maragos

Division of Applied Sciences, Harvard University, Cambridge, MA 02138

ABSTRACT - This paper reviews some recent advances in the theory and applications of morphological image analysis. In applications, we show how the morphological filters can be used to provide simple and systematic algorithms for image processing and analysis tasks as diverse as nonlinear image filtering; noise suppression; edge detection; region filling; skeletonization; coding; shape representation, smoothing, and recognition. In theory, we summarize the representation of a large class of translation-invariant nonlinear filters (including morphological, median, order-statistics, and shape recognition filters) as a minimal combination of morphological erosions or dilations; these results provide new realizations of these filters and lead to a unified image algebra.

1 Introduction

Digital image processing and analysis in the U.S.A. was developed from the 1960's motivated mainly by problems in remote sensing and scene analysis; its main mathematical tools included classical linear filters, Fourier analysis, and statistical or syntactic pattern recognition. Parallel to and independently from these ideas, **mathematical morphology** evolved in Europe from the 1960's as a set-theoretic method for image analysis motivated mainly by problems in quantitative microscopy; its mathematical tools are related to integral geometry and stereology. The theoretical foundations of mathematical morphology, its main image operations (which stem from Minkowski set operations [1,2]) and their properties, and a wide range of its applications were introduced systematically by Matheron [3] and Serra [4]. The image operations of mathematical morphology, which we call *morphological filters*, are more suitable for shape analysis than linear filters. Many of the well-established applications of morphological filters are in broad areas including biomedical image processing, metallography, geology, geography, remote sensing, astronomy, and automated industrial inspection [4,5,6,7,8].

Recently [9,10,11,12,13] mathematical morphology was applied to standard areas of macroscopic image processing and analysis such as nonlinear image filtering; edge detection; noise suppression; shape representation, smoothing, and recognition; skeletonization; coding; and the development of a theory for a unified image algebra. In this paper we shall briefly review these recent advances. Although, there are many different techniques for solving these problems (e.g., see [14,15,16] for reviews), our only aim is to show that a variety of tasks in image processing/analysis can be approached or solved using morphological concepts, and that many algorithms can be expressed compactly and systematically in terms of morphological filters.

2 General Concepts

In the Appendix we give the definitions of the basic morphological filters for *discrete* (i.e., sampled) images. These are nonlinear translation-invariant image or signal transformations that locally modify the *geometric* features of signals such as their peaks and valleys; they involve the interaction, through set operations, of the graph (and its interior) of signals and some compact sets of rather simple shape and size, called the *structuring elements*. To better understand the similarities and differences between morphological filtering of binary and graytone images, we use the following formalism.

Binary discrete images are represented by 2-D sets in the discrete plane $\mathbf{Z}^2$, where $\mathbf{Z}$ is the set of integers and $\mathbf{R}$ is the set of real numbers. Graytone discrete images are represented by 2-D functions whose domains are subsets of $\mathbf{Z}^2$ and ranges are subsets of $\mathbf{R}$. Thus, henceforth, **set** will imply a binary image, whereas **function** will refer to a graytone image. Since morphological filters are defined through set operations, the main concept here is *sets*. Hence, a 2-D graytone image function $f(x)$, $x \in \mathbf{Z}^2$, is also represented by a family of 2-D sets (binary images). That is, by *thresholding* f at all possible amplitudes $t \in \mathbf{R}$ we generate a family of 2-D sets

$$X_t(f) = \{x \in \mathbf{Z}^2 : f(x) \geq t\}, \quad t \in \mathbf{R}, \tag{1}$$

which are called the **cross-sections** of f. The sets $X_t(f)$ are decreasing as t increases; i.e., $t_2 \geq t_1 \Longrightarrow X_{t_2}(f) \subseteq X_{t_1}(f)$. Further, we can reconstruct exactly f if we know all its cross-sections [4,11]. Set union and intersection of the cross-sections of two functions f and g correspond, respectively, to the nonlinear function operations of **pointwise maximum** and **minimum**; i.e., $X_t(f) \cup X_t(g) = X_t(f \vee g)$ and $X_t(f) \cap X_t(g) = X_t(f \wedge g)$, where $(f \vee g)(x) = max[f(x), g(x)]$ and $(f \wedge g)(x) = min[f(x), g(x)]$. Set inclusion of cross-sections corresponds to an **ordering of functions**; i.e., $X_t(f) \subseteq X_t(g)\ \forall t \in \mathbf{R} \iff f \leq g$, where "$f \leq g$" denotes $f(x) \leq g(x)\ \forall x \in \mathbf{Z}^2$.

An image processing system whose input and output are

binary images is called a 2-D **set-processing (SP)** filter. Likewise, a system that transforms an input graytone to an output graytone image is called a 2-D **function-processing (FP)** filter. A subclass of FP filters can produce an output binary image when the input is also binary; these are called 2-D **function- and set-processing (FSP)** filters. We also use the same definitions for filters processing binary or multilevel signals of any dimensionality. Tables 1,2,3 in the Appendix give the definitions of various nonlinear SP, FP, or FSP filters.

The simplest SP morphological filters are the erosion, dilation, opening, and closing of a set by a *finite structuring set* (see Table 1). Figure 1 shows that erosion of a 2-D set X (binary image of an island) in $\mathbf{R}^2$ by a compact set B (a structuring disk) shrinks X, whereas dilation expands it. Erosion and dilation are *dual* filters; i.e., $X \oplus B = (X^c \ominus B)^c$. The opening and closing smooth the contours of X from the inside and outside, respectively, so that always $X_B \subseteq X \subseteq X^B$. Moreover, the opening suppresses the sharp capes and cuts the narrow isthmuses of the image object X, whereas the closing fills up its thin gulfs and small holes. Opening and closing are dual filters, because $X^B = [(X^c)_B]^c$.

Parallel to the evolution of all these morphological filters in [3,4], since the 1960's there have been many other researchers who have been using similar operations of the shrink/expand type (or cascades of shrink/expand's) for digital (binary) image processing and for cellular array computers designed for image analysis. (See [17,15] for surveys of these approaches.)

The morphological filters have been extended to functions too [4,5,6,11,18,19,20]. Table 2 contains the most general morphological FP filters; these involve the *morphological convolution* (max of sums and/or min of differences) of a function f with a *structuring function* g that has a *finite region of support*. However, the simplest morphological filters for graytone images, which have also received the most attention so far, are the FSP filters of Table 3. These FSP filters are the erosion (local min), dilation (local max), opening (local min/max), and closing (local max/min) of a 2-D function f by a 2-D *finite structuring set* A; they result as simple cases of the general FP filters of Table 2 by using a binary structuring function g whose region of support is equal to A. Figure 2 shows that the erosion of a function $f(x)$, $x \in \mathbf{Z}$, by a finite set $B \subseteq \mathbf{Z}$ broadens the minima of f, whereas dilation broadens the maxima. The opening of f by B cuts down the peaks of f, whereas the closing fills up its valleys, so that always $f_B \leq f \leq f^B$. Thus the FSP erosion and dilation of a function by a small set can detect the minima and maxima of the function; the FSP opening and closing can detect the peaks and valleys of the function, or suppress impulsive noise from signals in cases where the noise manifests itself as random patterns of positive and negative noise spikes.

All the FSP filters of Table 3 enjoy an important property: they **commute with thresholding**. That is, let ϕ denote such a FSP filter and let Φ denote its respective SP filter. Then, we say that ϕ commutes with thresholding iff

$$\Phi[X_t(f)] = X_t[\phi(f)] \ , \ \forall t \in \mathbf{R}, \qquad (2)$$

for all functions f. That is, if Φ is applied to all the cross-sections of f, then its outputs are identical to the cross-sections of the output of ϕ, where ϕ operates on the input f. In this way, the filtering of a multilevel signal reduces to a stack of filters for binary signals, which are easier to analyze and implement. For example, if $\phi(f) = f \oplus A$ is the FSP Minkowski function addition with A, its respective SP system is $\Phi(X) = X \oplus A$, i.e., the Minkowski set addition with A, and we have that $[X_t(f)] \oplus A = X_t(f \oplus A)$ $\forall t \in \mathbf{R}$.

Finally, examples and interpretations of morphological filtering of a function f by a multilevel structuring function g (i.e., the FP filters of Table 2, which *do not* commute with thresholding), as well as detailed properties of the basic SP and FP morphological filters can be found in [4,6,11,13,20].

3 Unified Image Algebra

In [10,11] we introduced a general theory to unify many concepts encountered in signal processing and image analysis and to represent a broad class of nonlinear and linear SP and FP filters as a minimal combination of morphological erosions or dilations. This theory applies to filters processing signals of any dimensionality and of both continuous and discrete argument or amplitude. However, in this paper we summarize (in a simplified way) the main results of this theory only for *discrete* images.

Consider any 2-D SP filter Ψ that is defined on the class $\mathcal{P}(\mathbf{Z}^2)$ of all subsets of $\mathbf{Z}^2$. The filter is called **translation-invariant (TI)** iff $\Psi(X_p) = [\Psi(X)]_p$, $\forall X \subseteq \mathbf{Z}^2$, $\forall p \in \mathbf{Z}^2$. Ψ is called **increasing** iff $A \subseteq B \Longrightarrow \Psi(A) \subseteq \Psi(B)$, for any $A, B \subseteq \mathbf{Z}^2$. An increasing SP filter Ψ is **upper semicontinuous (u.s.c.)** iff, for any decreasing sequence (X_n) of input sets (i.e., $X_{n+1} \subseteq X_n$), $\bigcap_n \Psi(X_n) = \Psi(\bigcap_n X_n)$. The **dual** (with respect to set complementation) filter of Ψ is defined as $\Psi^*(X) = [\Psi(X^c)]^c$, $X \subseteq \mathbf{Z}^2$. Any TI filter Ψ is uniquely characterized by its **kernel** that is defined in [3] as the (infinite) subclass $\mathcal{K}(\Psi) = \{X \subseteq \mathbf{Z}^2 : 0 \in \Psi(X)\}$ of input sets. The pair $(\mathcal{K}(\Psi), \subseteq)$ is a *partially ordered set* (*poset*) with respect to *set inclusion* $\subseteq$. A **minimal element** of $(\mathcal{K}(\Psi), \subseteq)$ is any set $G \in \mathcal{K}(\Psi)$ that is not preceded (with respect to $\subseteq$) by any other kernel set. In [10,11] we defined the **basis** $\mathcal{B}(\Psi)$ of the TI filter Ψ as the *set of all its minimal kernel elements*, and we showed that the basis *exists* (i.e., is nonempty) if Ψ is increasing and u.s.c. The importance of the basis is revealed by the following theorem.

THEOREM 1. [10,11] *(SP Filters). Let $\Psi : \mathcal{P}(\mathbf{Z}^2) \rightarrow \mathcal{P}(\mathbf{Z}^2)$ be a 2-D discrete SP filter that is TI, increasing, and u.s.c. Then Ψ can be represented exactly as the union of erosions by its basis sets. Further, if its dual filter Ψ^* is u.s.c., Ψ can be also represented exactly as the intersection of dilations by the basis sets of Ψ^*. That is, $\forall X \subseteq \mathbf{Z}^2$,*

$$\Psi(X) = \bigcup_{G \in \mathcal{B}(\Psi)} X \dot{\ominus} G^s = \bigcap_{H \in \mathcal{B}(\Psi^*)} X \oplus H^s \qquad (3)$$

We extended in [10,11] the kernel and basis representation to FP filters in the following way. Let ψ be a 2-D FP filter defined on the class $\mathcal{F}$ of all real-valued functions whose

domains are subsets of $\mathbf{Z}^2$. Then ψ is called **translation-invariant (TI)** iff $\psi[f(x-y)+c] = [\psi(f)](x-y)+c$, $\forall f(x) \in \mathcal{F}$, $\forall y \in \mathbf{Z}^2$, $\forall c \in \mathbf{R}$. That is, ψ is TI iff it commutes with a shift of both the argument and the amplitude of its input functions. Such a TI filter is uniquely characterized by its **kernel** that we defined as the (infinite) subclass $K(\psi) = \{f \in \mathcal{F} : [\psi(f)](0) \geq 0\}$ of input functions. The pair $(K(\psi), \leq)$ is a poset with respect to the *function ordering* $\leq$. A minimal function-element in $(K(\psi), \leq)$ is a function $g \in K(\psi)$ that is not preceded (with respect to function $\leq$) by any other kernel function. We defined the **basis** $B(\psi)$ of ψ as the set of its minimal kernel functions. A FP filter ψ is **increasing** iff $f \leq g \Longrightarrow \psi(f) \leq \psi(g)$, for any $f,g \in \mathcal{F}$. An increasing FP filter ψ is **u.s.c.** iff, for each decreasing sequence (f_n) of input functions (i.e., $f_{n+1} \leq f_n$) with $f(x) = \inf_n\{f_n(x)\}$ $\forall x$, we have that $[\psi(f)](x) = \inf_n\{[\psi(f_n)](x)\}$. The basis of any TI, increasing, u.s.c. FP filter *exists* and can exactly *represent* it, as explained below.

THEOREM 2. [10,11] *(a)-(Any FP filter). Let $\psi : \mathcal{F} \rightarrow \mathcal{F}$ be a 2-D discrete FP filter that is TI, increasing, and u.s.c. Then ψ can be represented exactly as the pointwise supremum of erosions by its basis functions; i.e., $\forall f \in \mathcal{F}$, $\forall x \in \mathbf{Z}^2$,*

$$[\psi(f)](x) = \sup_{g \in B(\psi)} \{(f \ominus g^s)(x)\} \tag{4}$$

(b)-(FSP filters). Let $\phi : \mathcal{F} \rightarrow \mathcal{F}$ be a FSP 2-D discrete TI filter and let Φ be its respective SP filter. If ϕ commutes with thresholding and the dual SP filter Φ^* is u.s.c., then ϕ can be represented exactly as the supremum of erosions by the basis sets of Φ and also as the infimum of dilations by the basis sets of Φ^*; i.e.,

$$\phi(f)(x) = \sup_{G \in B(\Phi)} \{f \ominus G^s(x)\} = \inf_{H \in B(\Phi^*)} \{f \oplus H^s(x)\} \tag{5}$$

Note that in Theorem 2b we omitted the assumptions about ϕ and Φ being increasing and u.s.c. The reason is that the assumption about ϕ being a TI FSP filter commuting with thresholding is sufficient to show that Φ is TI and that both ϕ and Φ are increasing and u.s.c.; hence Φ^* is also TI and increasing.

In the next section we will apply the general Theorems 1,2 to some special cases of nonlinear filters for discrete images.

4 Morphological, Median, and OS Filters

Median and, their generalization, *order-statistics (OS)* filters are nonlinear TI filters that have recently become popular for smoothing and enhancement of image and speech signals. (See [14,21] for reviews.) Let $W \subseteq \mathbf{Z}^2$ be a finite set with n points; i.e., $|\ W\ | = n$. As defined in Table 3, for $k = 1,2,\ldots,n$, the output of the FSP k-th OS filter by W at any location $x \in \mathbf{Z}^2$ is obtained by *sorting* at descending order the n values of the input function f inside the shifted window W_x and picking the k-th number from the sorted list. If n is odd and $k = (n+1)/2$ we have the special case of the **median** filter $med(f;W)$ of f by W. The respective OS and median SP filters are defined in Table 1; their definition involves only *counting* of points and no sorting.

The theoretical analysis of these useful filters becomes intractable beyond a small number of quantitative results, because all the well-known tools from the theory of linear filters do not apply here since these filters are nonlinear and have a nonzero memory. However, by using mathematical morphology and the theory of minimal elements (section 3), we developed in [10,11] a framework that facilitates the theoretical analysis of these filters, related them to morphological filters, and provided some new realizations for them. Specifically, from their definitions it is clear that the FSP or SP first ($k = 1$) OS filter by W is identical to the FSP or SP dilation by W; likewise, the last ($k = n$) OS filter is identical to the erosion by W. Further, OS and median filters commute with thresholding; e.g., $X_t[med(f;W)] = med[X_t(f);W]$, $\forall t \in \mathbf{R}$. The FSP morphological filters of Table 3 commute also with thresholding. This property allows us to study all the FSP filters of Table 3 for graytone images by focusing on their respective SP filters of Table 1 for binary images; further, the SP filters are easier to analyze and implement. From these general concepts we showed in [10,11] that

(A) All FSP filters of Table 3 and their respective SP filters of Table 1 are TI, increasing, and u.s.c. Hence their basis exists and exactly represents them through Theorems 1,2.

(B) Let $A \subseteq \mathbf{Z}^2$ be finite with $|\ A\ | = m$. The basis of the SP erosion by A has one element, the set A. The basis of the SP dilation by A has m elements, the one-point sets $\{a\}$ with $a \in A$. The basis of the SP opening by A has m elements, the sets A_{-a} with $a \in A$. The basis of the SP closing by A is the set of all minimal subsets M of $A \oplus A^s$ such that $0 \in M^A$.

(C) The basis of the SP k-th OS filter by $W \subseteq \mathbf{Z}^2$ ($|\ W\ | = n$) is the set of all subsets G of W with $|\ G\ | = k$. If n is odd, the basis of the SP median by W is the set of all subsets M of W with $|\ M\ | = (n+1)/2$. The dual filter of the SP k-th OS by W is the $(n-k+1)$-th OS filter by W. Thus, from Theorem 2b, $OS^k(f;W)$ is equal to the maximum of the local minima of f inside all $G \subseteq W$ with $|\ G\ | = k$ and also equal to the minimum of the local maxima of f inside all $H \subseteq W$ with $|\ H\ | = n-k+1$. For the median $med(f;W)$ we obtain the same representation with the only difference that the subsets G and H are identical because $k = (n+1)/2$.

(D) Let $A \subseteq \mathbf{Z}$ be convex with $|\ A\ | = n+1$, $n \geq 1$, and let $W \subseteq \mathbf{Z}$ be convex and symmetric ($W = W^s$) with $|\ W\ | = 2n+1$. Then, for any 1-D function $f(x)$, $x \in \mathbf{Z}$,

(i) Openings and closings by A are lower and upper *bounds* of medians by W; i.e., $f_A \leq med(f;W) \leq f^A$.

(ii) A finite extent signal f is a *fixed point* (*root*) of the median by W iff it is a root of the opening and closing by A; i.e., $f = f_A = f^A \Longleftrightarrow f = med(f;W)$.

(iii) Let $med^{(\infty)}(f;W)$ denote the *median root* obtained

by iterating (a finite number of times) the median filter by W on a finite extent 1-D signal f. Then the **open-closing** (opening followed by closing by the same set) $(f_A)^A$ and the **clos-opening** (closing followed by opening) $(f^A)_A$ are median roots with respect to W and they bound $med^{(\infty)}(f;W)$ since

$$f_A \leq (f_A)^A \leq med^{(\infty)}(f;W) \leq (f^A)_A \leq f^A$$

(iv) Similar results as in (i,ii) were obtained for 2-D opening/closing and median filters.

Next we illustrate some of the results in (A),(B),(C),(D) through the following simple example. Let $A = \{0,1\}$ and $W = \{-1,0,1\}$. Consider the SP opening $\Phi(X) = X_A$, $X \subseteq \mathbf{Z}$; its dual SP filter is the closing $\Phi^*(X) = X^A$. Then the basis of Φ has two minimal elements, the sets $\{0,1\}$ and $\{-1,0\}$. The basis of Φ^* has two elements, the sets $\{0\}$ and $\{-1,1\}$. Thus, from Theorem 2b, the FSP opening $\phi(f) = f_A$ is a maximum of erosions by the basis sets of Φ and a minimum of dilations by the basis sets of Φ^*; i.e.,

$$\begin{aligned} f_A(x) &= \max\{\min[f(x-1), f(x)] \,,\, \min[f(x), f(x+1)]\} \\ &= \min\{f(x) \,,\, \max[f(x-1), f(x+1)]\} \end{aligned} \tag{6}$$

for any function $f(x)$, $x \in \mathbf{Z}$. Since opening and closing are dual filters, if we interchange max and min everywhere in (6) we obtain a formula for the closing f^A. The basis of the SP median by W has three elements, the sets $\{-1,0\}$, $\{-1,1\}$ and $\{0,1\}$. Thus, from Theorem 2b,

$$med[f(x-1), f(x), f(x+1)] = \max \left\{ \begin{matrix} \min[f(x-1), f(x)] \\ \min[f(x-1), f(x+1)] \\ \min[f(x), f(x+1)] \end{matrix} \right\} \tag{7}$$

Because the SP median is equal to its dual filter, we can interchange min and max in (7). From (6) and (7) it follows that $f_A \leq med(f;W) \leq f^A$, in agreement with result (D-i).

Figure 3 compares the nonlinear smoothing results of 1-D open-closings, clos-openings, and iterated medians. Figure 3a shows an original 1-D function (an image intensity profile) containing many narrow peaks and valleys; Figs. 3b,c show the open-closing and clos-opening of f by a 3-points set L; Fig. 3d shows the median root g obtained by iterating four times a median filter by a 5-points window B. The open-closing (and clos-opening) by L is a median root with respect to B, smooths the signal very similarly to the median root g, lies close to g, and is computationally much less complex [11] than iterating the median by B.

5 Edge Detection [4,5,11,12]

Let B be one of the *unit-size* structuring elements of Fig. 4. Then

$$nB = B \oplus B \oplus \ldots \oplus B \quad (n \text{ times})$$

denotes an element of *size* n, where n is any nonnegative integer. If B is convex, then nB has the same shape as B; if $n = 0$, then nB is just the one-point set $\{0\}$. If B is 2-D symmetric, then the set difference $X - (X \ominus nB)$ gives the boundary of a binary image X, and the algebraic difference $f - (f \ominus nB)$ enhances the edges of a graytone image f, as Fig. 5 shows. The size n of nB controls the *thickness* of the edge-markers. Edges in different orientations can be obtained by using a 1-D structuring set B properly oriented. A more symmetric treatment between the image and its background would be the edge-estimator $(f \oplus nB) - (f \ominus nB)$, which approximates the gradient of f [4].

6 Noise Suppression

Figure 6a shows a graytone image f corrupted by *salt-and-pepper* noise. Figure 6b shows the opening f_B (B=*boxne* of Fig. 4), which cuts down the positive noise spikes. The negative noise spikes are cleaned (filled up) by the open-closing $(f_B)^B$, as shown in Fig. 6c. The cleaning effects of the open-closing are comparable to the median filtering (see Fig. 6d) of f by the window W=*square* of Fig. 4. However, the open-closing by B is computationally less complex than the median by W and can decompose the noise suppression into two separate tasks: cleaning of the positive or negative spikes (see also Fig. 2). Related approaches to image cleaning from impulsive noise can be found in [4,5,6,15,17,18,19].

7 Region Filling

We present here a compact algorithm [11,12] for region filling that requires only set dilations, complementation, and intersections. Figure 7a shows the boundaries of two disjoint regions, whose union represents a binary image X. The problem is to fill in (*paint*) the interior of the left region (call it set F) if we know a point p inside it. Figure 7b shows the complement of X. Let $B \supseteq \{0\}$ be a symmetric structuring element whose half diameter does not exceed the width of the boundary. If $Y^0 = \{p\}$ and

$$Y^i = (Y^{i-1} \oplus B) \cap X^c, \quad i = 1,2,3,\ldots,$$

then the filled interior is given in general by $F = Y^\infty$. Thus, the dilation tends to fill the whole area, whereas the intersection with X^c limits the result inside the left region. Of course, practically we need only a finite number of iterations to find F, since the condition $Y^{i+1} = Y^i$ signals that the region F has been fully painted. Figure 7d shows the fully painted left region after only eighteen iterations of the above algorithm. (Fig. 7c shows the intermediate result after the 8-th iteration.)

8 Skeletonization, Shape Smoothing, Coding

The skeleton (or *medial axis*) of a finite discrete binary image X has been extensively studied and used for image analysis. (See [22,15,16] for reviews.) In [4,23,11,13] and indirectly in [24] it was shown that the skeleton can be obtained by erosions and openings. Specifically, if B is any discrete

structuring element with $0 \in B$, then the **morhological skeleton**, $SK(X)$, of X (with respect to B) is the finite union of disjoint **skeleton subsets** $S_n(X)$; i.e.,

$$SK(X) = \bigcup_{0 \le n \le N} S_n(X) \tag{8}$$

where

$$S_n(X) = (X \ominus nB^s) - (X \ominus nB^s)_B \tag{9}$$

and $n = 0, 1, 2, \ldots, N = \max\{k : X \ominus kB^s \neq \emptyset\}$. The image X can be reconstructed as the union of all the skeleton subsets dilated by an element of proper size; i.e.,

$$X = \bigcup_{0 \le n \le N} [S_n(X) \oplus nB] \,. \tag{10}$$

If the first k lower-indexed skeleton subsets are omitted in (10), then we reconstruct the opening of X by kB; i.e.,

$$X_{kB} = (X \ominus kB^s) \oplus kB = \bigcup_{k \le n \le N} [S_n(X) \oplus nB] \,. \tag{11}$$

If B is convex, these openings X_{kB} represent *smoothed* versions of X, where the degree of smoothness depends only on the *size* k of kB; i.e., the larger the size k, the smoother the opening X_{kB}. Because X can be reconstructed either *exactly* from all $S_n(X)$ using (10) or *partially* (smoothed versions) using (11), we can view the skeleton subsets as "*shape components*". That is, skeleton subsets of small indices n are associated with the lack of smoothness of the boundary of X, whereas skeleton subsets of large indices n are related to the bulky interior parts of X that are shaped similarly to nB. Thus (10) and (11) imply that an arbitrary shape X is smooth to a degree k with respect to a fixed shape B (i.e., $X = X_{kB}$) if the first k shape components of X (i.e., first k $S_n(X)$) are empty. The converse, i.e., $X = X_{kB} \Longrightarrow S_n(X) = \emptyset$ for $0 \le n \le k-1$ is true if both X and B are convex [13].

Symmetric (disk-like) structuring elements produce a skeleton that looks like a "symmetry axis". At the expense of loosing this property, we can use the above morphological skeletal decomposition and reconstruction algorithms with an asymmetric, or even a 1-D, element. Figure 8 illustrates the variety of skeletons that result from varying the structuring element. It also shows the ability of morphological filters to extract different structural information by using different structuring elements. One application for asymmetric or 1-D structuring elements for skeletonization was described in [11,13], where we searched for the element giving the skeleton with fewest points, and hence lowest information rate required to encode the image.

All the skeletons of Fig. 8 can reconstruct X and retain some of the axial character of a skeleton. However, they may be redundant. Thus, at the expense of producing a skeleton that may not look like a skeletal axis, we defined the **minimal skeleton** to be a proper subset of the original skeleton whose points are sufficient for exact reconstruction, but removal of just one point would result in partial reconstruction. In [11,13] we provided a fast algorithm that finds such a minimal skeleton, if it exists. Figure 9 shows two original binary images of different spatial resolution together with their original and minimal skeletons.

In [11,13] we showed that encoding of the minimal skeleton information using Elias codes results in higher compression than either optimum block-Huffman or optimum runlength-Huffman coding of the original image. Figure 10 shows an application of simultaneous skeleton coding and morphological smoothing of a binary image X. By eliminating the first skeleton subset $S_0(X)$ and encoding the rest skeleton subsets (thus reconstructing the opening X_B) the original information of 65.5Kbits in X and X_B was compressed down to 5.7Kbits; i.e., a compression ratio of 11.4:1. Further decimation of X by keeping one out of every 4×4 pixels and skeleton-encoding of the decimated image compresses the information down to 1.2Kbits; i.e., a compression ratio of 53:1. In addition, morphological post-filtering can smooth the jagged contours of the interpolated image.

Finally, the morphological skeletonization has been extended to multilevel signals (e.g., graytone images) in [25] and in [11].

9 Shape Recognition

Minimal Skeletons. The minimal skeleton was also used for minimal shape representation and recognition of blob-shaped images in [11]. That is, consider the problem: "*Given a fixed convex shape B, find a minimum number of maximal scaled and shifted versions, $(nB)_z$, of B (i.e., find their locations z and sizes n) that fit inside an image object X and whose union exactly represents X.*" Since the morphological skeletonization of X by B gives all the locations and sizes of maximal elements $(nB)_z$ whose union reconstructs X, the minimal skeleton gives, by definition, an exact solution to the above problem. Figure 11a shows a discrete binary image X that was formed as the union of three elements nB (B=*circle* of Fig. 4), two of size $n = 1$ and one of size $n = 2$; its original skeleton with respect to B has eight points. Its minimal skeleton (in Fig. 11b) contains only the three centers, recognizing thus the existence, location, and size of the three overlapping blobs. Thus both skeletons can reconstruct X exactly, but the the minimal skeleton displays clearly that the composite shape X consists of three simpler blobs.

Hit-or-miss transforms. Let X be an image object and A a fixed structuring element; e.g., Fig. 12 shows an object X consisting of three disks of different radii, and A is the medium size disk. Suppose now that W is a small window surrounding A. The *local background* of A with respect to W is the set difference $(W - A)$. The set of locations at which A *exactly fits* inside X, denoted by $SR_W(X; A)$, is the intersection of the erosion of X by A and the erosion of X^c by $W - A$ (see Fig. 12). This set transform uses erosion as a *matched filter* for shape recognition; it was introduced in [26] and was shown to be the prototype of a class of TI image transforms for pattern recognition. However, this transform is a special case of the general morphological hit-or-miss transform defined in Table 1; i.e., $SR_W(X; A) = X \odot (A, B)$ with $B = W - A$. Based on this latter observation we showed in [11] that such *increasing* pattern recognition transforms

can be realized more efficiently (computationally) via erosions by their minimal elements.

10 Discussion

We have only mentioned a few among the numerous applications of morphological filters to image processing/analysis. A much broader spectrum of applications and algorithms in image processing/analysis expressed using morphological concepts and filters can be found in [4] and in the references of [11,12,13,20]. These illustrations demonstrate the utility of such image operations and thus the potential value of the unified image algebra that we developed in [10,11] to encompass a broad class of such systems. That is, we have theoretically founded all these evidences by showing that morphological erosions and dilations are the prototypes of a large class of nonlinear filters processing binary or graytone images and signals. We call this unified image algebra the *theory of minimal elements*, because filters are realized as a *minimal* combination of morphological convolutions with some characteristic input signals, i.e., the minimal elements. Among the filters that this theory unifies we examined here some morphological, median, and OS filters; in [11] we also applied the theory to classical *linear* filters and shape recognition transforms. In short, this unifying theory is attractive because:

1) It is developed for the large class of TI, increasing, u.s.c. filters, whose importance is profound in image processing and analysis. Moreover, some TI systems that are not increasing, e.g., the skeleton, or the hit-or-miss transform, can be expressed as the difference of two TI increasing systems.

2) It provides *new realizations* of many nonlinear and linear filters. For example, 1-D openings and closings were implemented faster by using the minimal elements of their dual filters; median and OS filters were expressed through a closed formula involving min/max on prespecified sets of numbers and no sorting. Some of these new realizations could have been derived by using combinatorial proofs, which we provided in [11]. However, there was a total lack of similarity in these proofs and a need for inventing new "tricks" in each case. This contrasts unfavourably with the generality of the theory of minimal elements, from which the special cases result as simple corollaries.

3) The prototype filters of this theory are *simple* and attractive for *parallel implementation.* That is, erosions or dilations by sets can be simply implemented as a parallel logical AND or OR of shifted versions of the input signal [27,11,13]. There are also many commercialized computer architectures that implement morphological filters; references can be found in [4,6,11,20].

4) Erosions, dilations, and the rest of morphological filters (which are combinations of erosions or dilations) are defined by logical operations on sets representing signals. This makes them well-suited for shape analysis or extraction of geometrical and topological features from signals or image objects. It also helps to obtain the solution of a class of problems directly from their statement as a morphological operation. Moreover, morphological filters are based on the principles of mathematical morphology which is an area rich in concepts and mathematical formalism. All these factors create an interesting circle of ideas and problems to which the theory of minimal elements applies.

5) The theory can lead to synthesis and design of new systems.

6) From this unified image algebra autonomous *machine vision modules* could be designed, which could perform a large variety of complex image processing/analysis tasks based on a small set of simple and parallel image operations.

Concluding, for future work there are still many issues yet to be investigated. For example, systematic general algorithms are needed for obtaining the basis of an arbitrary filter and for determining in advance whether it contains a finite or infinite number of minimal elements. The synthesis of systems based on their minimal elements remains an open area. Finally, there is a total lack of analytic criteria to design the generalized morphological filters for graytone images of Table 2 and thus solve more complex image processing tasks.

11 Appendix

Here we define the morphological filters only for *discrete* images defined on $\mathbf{Z}^2$. (The notation $\{x : \mathrm{P}\}$ is used everywhere to denote the set of points x satisfying a property P.) To obtain the respective definitions for non-sampled images defined on the continuous plane $\mathbf{R}^2$, the reader must replace in Tables 2,3 the maximum with supremum and the minimum with infimum, and assume that the structuring set A is compact and the structuring function g has a compact region of support.

Table 1: **SP Filters for Binary Discrete Images**

Name	Definition*
set translation of A by p	$A_p = \{p + a : a \in A\}$
set symmetric of A	$A^s = \{-a : a \in A\}$
set difference of B from A	$A - B = \{a : a \in A,\ a \notin B\}$
set complement of A	$A^c = \{a \in \mathbf{Z}^2 : a \notin A\} = \mathbf{Z}^2 - A$
Minkowski set addition of A and B	$A \oplus B = \{a + b : a \in A,\ b \in B\} = \bigcup_{b \in B} A_b$
Minkowski set subtraction of B from A	$A \ominus B = (A^c \oplus B)^c = \bigcap_{b \in B} A_b$
dilation of X by A	$X \oplus A^s = \{p \in \mathbf{Z}^2 : A_p \cap X \neq \emptyset\}$
erosion of X by A	$X \ominus A^s = \{p \in \mathbf{Z}^2 : A_p \subseteq X\}$
closing of X by A	$X^A = (X \oplus A^s) \ominus A$
opening of X by A	$X_A = (X \ominus A^s) \oplus A$
hit-or-miss transform of X by (A, B)	$X \odot (A, B) = (X \ominus A^s) \cap (X^c \ominus B^s)$
k-th order-statistic of X by W	$OS^k(X; W) = \{p \in \mathbf{Z}^2 : \mid X \cap W_p \mid \geq k\}$
median of X by W ($\mid W \mid = n$ =odd)	$med(X; W) = OS^{(n+1)/2}(X; W)$
* $X, A, B, W \subseteq \mathbf{Z}^2$; $p \in \mathbf{Z}^2$	* $\mid W \mid$=cardinality of W

Table 2: **FP Filters for Graytone Discrete Images**

Name	Definition ($x, y \in \mathbf{Z}^2$)
function symmetric of g(x)	$g^s(x) = g(-x)$
Minkowski function addition of f and g	$(f \oplus g)(x) = \max\{f(y) + g(x - y) : y \in \mathbf{Z}^2\}$
Minkowski function subtraction of g from f	$(f \ominus g)(x) = \min\{f(y) - g(x - y) : y \in \mathbf{Z}^2\}$
dilation of f by g	$(f \oplus g^s)(x) = \max\{f(y) + g(y - x) : y \in \mathbf{Z}^2\}$
erosion of f by g	$(f \ominus g^s)(x) = \min\{f(y) - g(y - x) : y \in \mathbf{Z}^2\}$
closing of f by g	$f^g(x) = [(f \oplus g^s)(x)] \ominus g(x)$
opening of f by g	$f_g(x) = [(f \ominus g^s)(x)] \oplus g(x)$

Table 3: **FSP Filters for Graytone and Binary Discrete Images**

Minkowski addition of f and A	$(f \oplus A)(x) = \max\{f(y) : y \in (A^s)_x\}$
Minkowski subtraction of A from f	$(f \ominus A)(x) = \min\{f(y) : y \in (A^s)_x\}$
dilation of f by A	$(f \oplus A^s)(x) = \max\{f(y) : y \in A_x\}$
erosion of f by A	$(f \ominus A^s)(x) = \min\{f(y) : y \in A_x\}$
closing of f by A	$f^A = (f \oplus A^s) \ominus A$
opening of f by A	$f_A = (f \ominus A^s) \oplus A$
k-th OS of f by W	$[OS^k(f; W)](x) = k$-th largest of $f(y)$, $y \in W_x$
median of f by W	$med(f; W) = OS^{(n+1)/2}(f; W)$

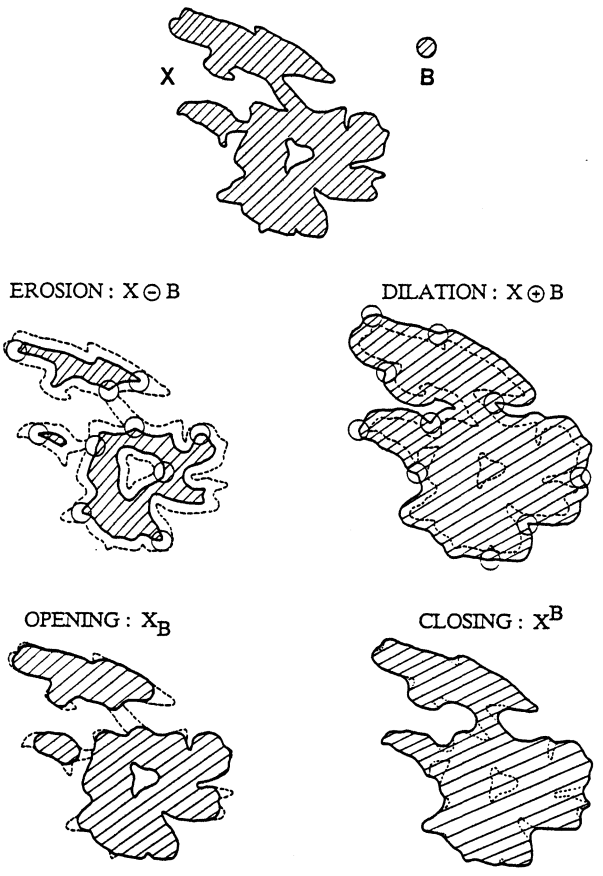

Figure 1. Erosion, dilation, opening, and closing of X by B. (The shaded areas correspond to the interior of the sets, the dark solid curve to the boundary of the transformed sets, and the dashed curve to the original boundary of X.)

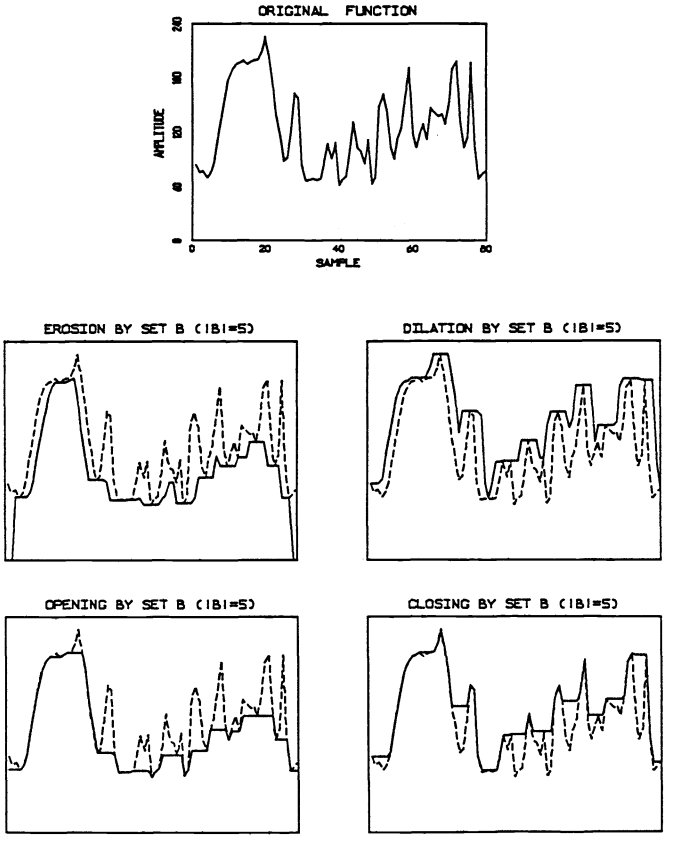

Figure 2. Erosion, dilation, opening, and closing of a 1-D sampled function by a 1-D set B. ($B = \{-2,-1,0,1,2\}$; the dashed curve refers to the original function.)

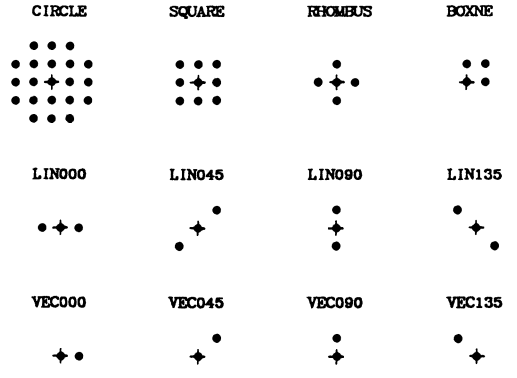

Figure 4. Discrete structuring elements in $\mathbf{Z}^2$. (+ marks the origin $(0,0)$ of $\mathbf{Z}^2$.)

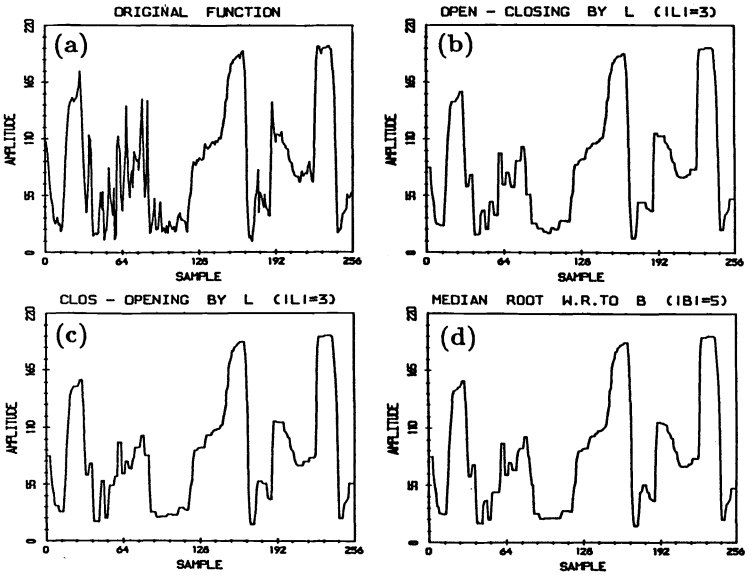

Figure 3. Median filtering via opening-closing: (a) Original function f. (b) Open-closing $(f_L)^L$. (c) Clos-opening $(f^L)_L$. (d) Median root of f by B. ($L = \{-1,0,1\}$ and $B = \{-2,-1,0,1,2\}$)

Figure 5. (a) A binary image X. (b) $X-(X\ominus B)$. (c) A graytone image f. (d) $f-(f\ominus B)$. (B=*circle* of Fig. 4.)

Figure 6. (a) An image f with *salt-and-pepper* noise (probability of occurrence of noisy samples is 0.1). (b) Opening f_B. (c) Open-closing $(f_B)^B$. (d) Median of f by the window W. (B=*boxne* and W=*square* of Fig. 4.)

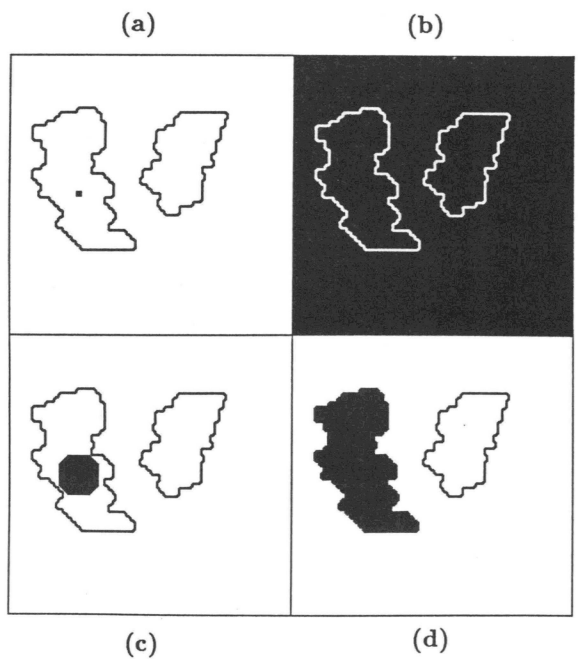

Figure 7. Region filling by dilation and intersections. (All images have 256 × 256 pixels.)

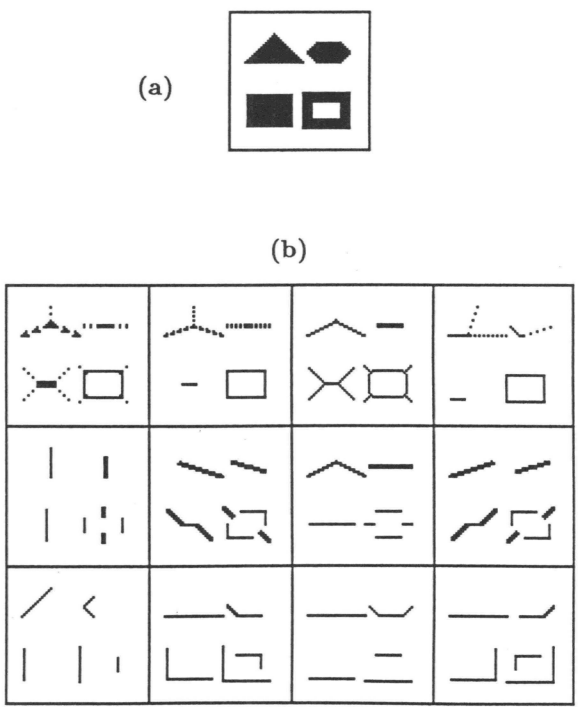

Figure 8. (a) A 64 × 64-pixels binary image. (b) Its morphological skeletons with respect to all the structuring elements of Fig. 4 (keeping the same order).

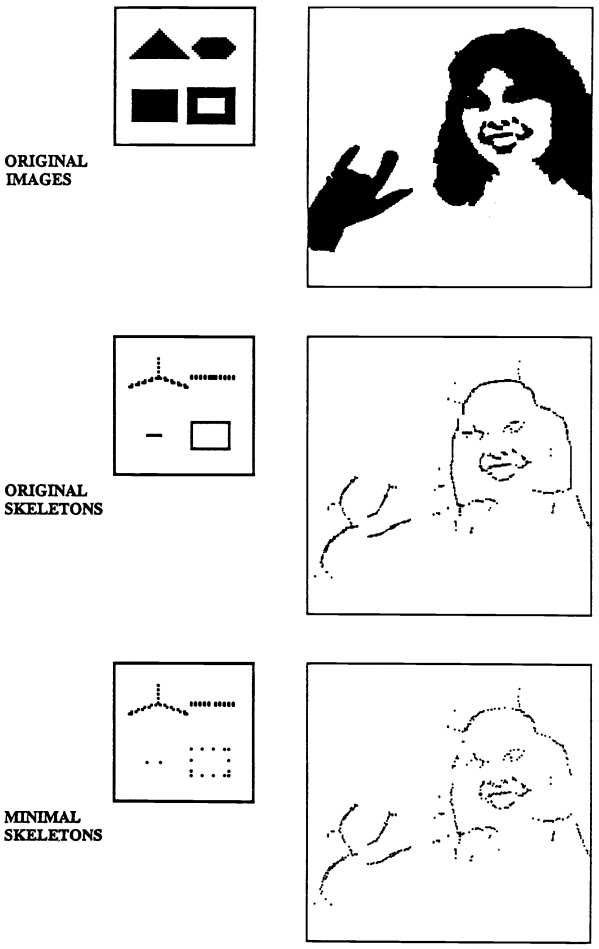

Figure 9. Minimal skeletonization (by the *square* of Fig. 4). (The (enlarged) images on the left have 64×64 pixels; images on the right have 256×256 pixels.)

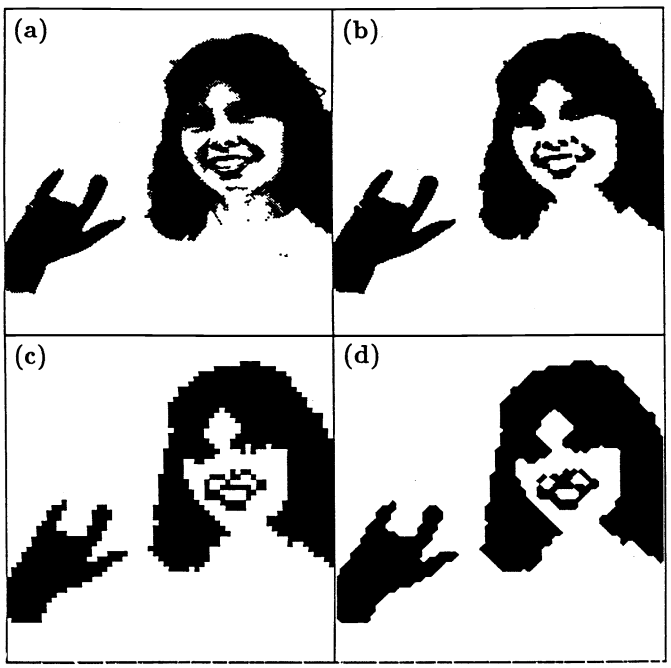

Figure 10. (a) Original binary image X (256×256 pixels resolution). (b) Opening X_B by B=*square* of Fig. 4. (Image data=65536 bits; after skeleton coding, 5734 bits.) (c) Image Y obtained by 4×4-decimating X and then 4×4-interpolating it back. (Image data=4096 bits; after skeleton coding, 1246 bits.) (d) Clos-opening $(Y^{2A})_{2A}$, where A=*rhombus* of Fig. 4.

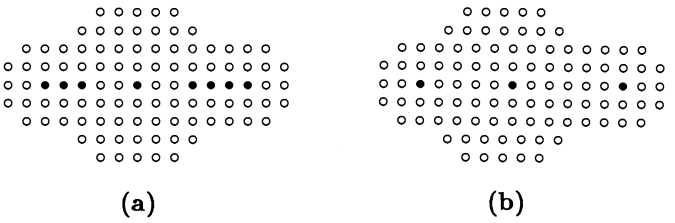

Figure 11. Minimal shape representation and blob recognition. (○, • = image points; • = skeleton points.)

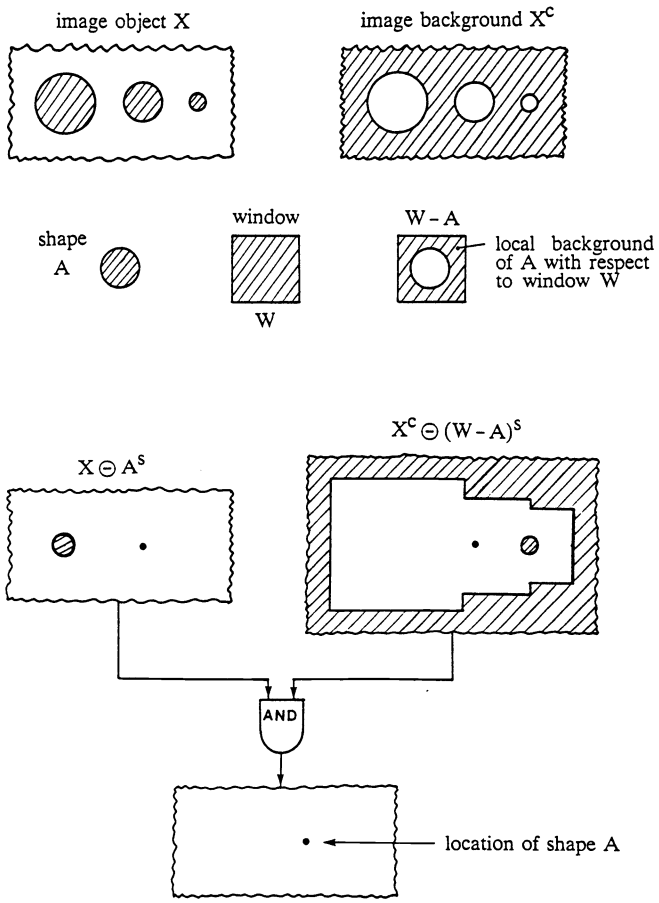

Figure 12. A shape recognition transform (adapted from Crimmins & Brown [26]).

Acknowledgments

This work was supported by the National Science Foundation under Contract CDR-8500108.

References

[1] H. Minkowski, "Volumen und Oberflache", *Math. Annalen*, Vol. 57, pp.447-495, 1093.

[2] H. Hadwiger, *Vorlesungen uber Inhalt, Oberflache, und Isoperimetrie*, Berlin: Springer Verlag, 1957.

[3] G. Matheron, *Random Sets and Integral Geometry*, NY: Wiley, 1975.

[4] J. Serra, *Image Analysis and Mathematical Morphology*, NY: Acad. Press, 1982.

[5] V. Goetcherian, "From Binary To Grey Tone Image Processing Using Fuzzy Logic Concepts," *Pattern Recognition*, Vol. 12, pp.7-15, 1980.

[6] S.R. Sternberg, "Biomedical Image Processing", *IEEE Computer*, Jan. 1983, pp.22-34.

[7] S.R. Stenrberg and E.S. Sternberg, "Industrial Inspection by Morphological Virtual Gauging", *Proc. IEEE Workshop Comp. Archit. for Pattern Anal. Image Datab. Manag.*, Pasadena CA, Oct. 1983.

[8] J.R. Mandeville, "Novel Method for Analysis of Printed Circuit Images", *IBM J. Res. Develop.*, 29, Jan. 1986.

[9] P. Maragos and R.W. Schafer, "Morphological Skeleton Representation and Coding of Binary Images", *Proc. IEEE Int. Conf. Acoust., Speech, Signal Processing*, San Diego CA, April 1984, pp.29.2.1-29.2.4.

[10] P. Maragos and R.W. Schafer, "A Unification of Linear, Median, Order-Statistics, and Morphological Filters under Mathematical Morphology", *Proc. IEEE Int. Conf. Acoust., Speech, Signal Processing*, Tampa FL, March 1985, pp.34.8.1-34.8.4.

[11] P. Maragos, *A Unified Theory of Translation-Invariant Systems With Applications to Morphological Analysis and Coding of Images*, Ph.D. Thesis, School of Electr. Enginr., Georgia Inst. of Technology, Atlanta GA, July 1985; also as *Tech. Rep. DSPL-85-1.*

[12] P. Maragos and R.W. Schafer, "Applications of Morphological Filtering to Image Analysis and Processing", *Proc. IEEE Int. Conf. Acoust., Speech, Signal Processing*, Tokyo Japan, April 1986, pp.2067-2070.

[13] P. Maragos and R.W. Schafer, "Morphological Skeleton Representation and Coding of Binary Images", to appear in *IEEE Trans. Acoust., Speech, Signal Processing*, Oct. 1986.

[14] W.K. Pratt, *Digital Image Processing*, NY: Wiley, 1978.

[15] A. Rosenfeld and A.C. Kak, *Digital Picture Processing*, Vols. 1 & 2, NY: Acad. Press, 1982.

[16] T. Pavlidis, *Algorithms for Graphics and Image Processing*, Computer Science Press, 1982.

[17] K. Preston, Jr., M.J.B. Duff, S. Levialdi, P.E. Norgren, and J-I. Toriwaki, "Basics of Cellular Logic with Some Applications in Medical Image Processing", *Proc. IEEE*, Vol. 67, pp.826-856, May 1979.

[18] Y. Nakagawa and A. Rosenfeld, "A Note on the Use of Local Min and Max Operations in Digital Picture Processing", *IEEE Trans. Syst., Man, and Cybern.*, Vol. SMC-8, Aug.1978, pp.632-635.

[19] C. Lantuejoul and J. Serra, "M-Filters," *Proc. IEEE Int. Conf. Acoust., Speech, Signal Processing*, Paris France, May 1982, pp.2063-2066.

[20] R.M. Haralick, S.R. Sternberg and X. Zhuang, "Gray-scale Morphology", *Proc. IEEE Comp. Soc. Conf. Comp. Vision Pattern Recogn.*, Miami FL, June 1986.

[21] T.S. Huang, Ed., *Two-Dimensional Digital Signal Processing II: Transforms and Median Filters*, NY: Springer Verlag, 1981.

[22] H. Blum, "Biological Shape and Visual Sciences (Part I)", *J. Theor. Biology*, Vol. 38, pp.205-287, 1973.

[23] C. Lantuejoul, "Skeletonization in Quantitative Metallography", in *Issues of Digital Image Processing*, R.M. Haralick & J.C. Simon, Eds., Sijthoff & Noordhoff, 1980.

[24] J.C. Mott-Smith, "Medial Axis Transformations", in *Picture Processing and Psychopictorics*, B.S. Lipkin and A. Rosenfeld, Eds., NY: Acad. Press, 1970.

[25] S. Peleg and A. Rosenfeld, "A Min-Max Medial Axis Transformation", *IEEE Trans. Pattern Anal. Machine Intellig.*, Vol. PAMI-3, pp.208-210, Mar. 1981.

[26] T.R. Crimmins and W.R. Brown, "Image Algebra and Automatic Shape Recognition", *IEEE Trans. Aerosp. and Electron. Syst.*, Vol. AES-21, pp.60-69, Jan. 1985.

[27] S.R. Sternberg, "Parallel Architectures for Image Processing", *Proc. IEEE Int. Comp. Softw. Appl. Conf.*, Chicago IL, 1979, pp.712-717.